

Available online at [www.sciencedirect.com](http://www.sciencedirect.com)

SCIENCE @ DIRECT®

Physics Letters B 629 (2005) 1–8

PHYSICS LETTERS B

[www.elsevier.com/locate/physletb](http://www.elsevier.com/locate/physletb)

# SnIa constraints on the event-horizon thermodynamical model of dark energy

J. Gariel, G. Le Denmat, C. Barbachoux

*LERMA, UMR CNRS 8112, Université P. et M. Curie ERGA, B.C. 142, 3, Rue Galilée, 94 200 Ivry, France*

Received 19 July 2005; received in revised form 12 September 2005; accepted 23 September 2005

Available online 29 September 2005

Editor: M. Cvetič

## Abstract

We apply the thermodynamical model of the cosmological event horizon of the spatially flat FLRW metrics to the study of the recent accelerated expansion phase and to the coincidence problem. This model, called “ehT model” hereafter, led to a dark energy (DE) density  $\Lambda$  varying as  $r^{-2}$ , where  $r$  is the proper radius of the event horizon. Recently, another model motivated by the holographic principle gave an independent justification of the same relation between  $\Lambda$  and  $r$ . We probe the theoretical results of the ehT model with respect to the SnIa observations and we compare it to the model deduced from the holographic principle, which we call “LHG model” in the following. Our results are in excellent agreement with the observations for  $H_0 = 64 \text{ km s}^{-1} \text{ Mpc}^{-1}$ , and  $\Omega_\Lambda^0 = 0.63_{-0.01}^{+0.1}$ , which leads to  $q_0 = -0.445$  and  $z_T \simeq 0.965$ .

© 2005 Elsevier B.V. Open access under [CC BY license](https://creativecommons.org/licenses/by/4.0/).

*Keywords:* Dark energy theory; Supernova type Ia

## 1. Introduction

Since the discovery of the presently accelerated expansion of the universe from supernovae observations [1,2], evidences for such an accelerated phase are increasing. The simplest theoretical candidate to explain this acceleration is a cosmological “constant”  $\Lambda$ . Anything producing sufficient negative pressure—for in-

stance a scalar field [3] or a bulk viscosity [4]—could also be valid.

Before the discovery of this acceleration, phenomenological ansätze with a variable  $\Lambda(t)$  were tentatively proposed as solutions of the cosmological “constant” problem (e.g., [5–11]).

From a different point of view, the generalization [12,13] of the black hole and of the de Sitter event-horizon thermodynamics [14,15] to the Friedmann–Lemaître–Roberston–Walker (FLRW) space–time has led to the relation  $\Lambda(t) \sim r^{-2}(t)$  [16] where  $r$  denotes the event-horizon in the FLRW model of the universe.

*E-mail addresses:* [gariel@ccr.jussieu.fr](mailto:gariel@ccr.jussieu.fr) (J. Gariel), [gele@ccr.jussieu.fr](mailto:gele@ccr.jussieu.fr) (G. Le Denmat), [barba@ccr.jussieu.fr](mailto:barba@ccr.jussieu.fr) (C. Barbachoux).

This model will be called the event horizon thermodynamical model (ehT model) hereafter.

Recently, this last form for  $\Lambda(t)$ , or, equivalently, for the dark energy density  $\rho_\Lambda(t)$  through  $\rho_\Lambda(t) = \chi^{-1}\Lambda(t)$  (with  $\chi = 8\pi Gc^{-4}$ ), has received further supports based on the holographic principle [17,18]. The associated model will be referred to as the LHG model in the following.

A model such that  $\Lambda \sim r^{-2}$  for the DE density can be used in different ways and different contexts. For instance, in a precedent paper [16] in order to address the problem of the exit of inflation in the early universe, we imposed as second component a perfect fluid of strings ( $\gamma = 2/3$ ). The model led then to  $\Lambda = 3\frac{\ddot{a}}{a}$ , which was independently considered as an ansatz by some authors [19–22].

In the present Letter, in order to settle some issues on the coincidence and the recent deceleration–acceleration transition problems, we assume for the second component a cold dark matter ( $P = 0$ ). In Section 2, we review some basic equations and relations common to the ehT and LHG models. The ehT model is developed in Section 3, particularly for the  $z \leq 2$  epoch. In Section 4, in order to probe the DE assumption in this range of  $z$ , we discuss how our model fits in with the type Ia supernovae recent observations [23]. We deduce then the most likely values for the  $H_0$  and  $\Omega_\Lambda^0$  parameters, as well as the deceleration parameter  $q_0$  and the deceleration–acceleration transition redshift  $z_T$ . Finally, Sections 5 and 6 contain comments and a brief comparative discussion concerning the results obtained by the two models.

## 2. Model for $\Lambda$ and field equations

In order to set the notations, we introduce some basic equations of the two-component models. The spatially flat FLRW space–time has the metric

$$ds^2 = c^2 dt^2 - a^2(t)[dR^2 + R^2(d\theta^2 + \sin^2\theta d\phi^2)], \quad (1)$$

where the scale factor  $a(t)$  is a monotonic increasing function of the cosmic time  $t$ .

We assume an universe filled by two type-like perfect fluids, namely dust (ordinary and dark matter) and dark energy (DE) with a type-like perfect fluid energy–

momentum tensor

$$T^{\alpha\beta} = \rho_{\text{tot}}u^\alpha u^\beta - P_{\text{tot}}\Delta^{\alpha\beta}, \quad \Delta^{\alpha\beta} = g^{\alpha\beta} - u^\alpha u^\beta, \quad (2)$$

where  $u^\alpha$  is the 4-velocity common to all the components of the energy density  $\rho_{\text{tot}}$ . We consider two components such as  $\rho_{\text{tot}} = \rho + \rho_\Lambda$  and  $P_{\text{tot}} = P + P_\Lambda$ . The first component ( $\rho, P$ ) is the matter with  $\rho$  the energy density,  $P$  the pressure and obeys the barotropic state equation  $P = (\gamma - 1)\rho$  where  $\gamma = \text{const}$ ,  $0 < \gamma \leq 2$  (for instance,  $\gamma = 1$  for dust). The second component is the dark energy (DE), with  $\rho_\Lambda = \chi^{-1}\Lambda$  the vacuum energy density and  $P_\Lambda$  the pressure, satisfying the state equation

$$P_\Lambda = \omega\rho_\Lambda, \quad (3)$$

where  $\omega$  ( $-1 \leq \omega < 0$ ) can be variable. The present results are valid for any first component of matter, namely any value of  $\gamma$ . In the next section, we will restrict our discussion to the particular case  $\gamma = 1$  corresponding to dust.

The field equations for the spatially flat case are

$$3H^2 = \chi c^2(\rho + \rho_\Lambda), \quad (4)$$

$$2\frac{\ddot{a}}{a} + H^2 = -\chi c^2(P + P_\Lambda), \quad (5)$$

where  $H \equiv \frac{\dot{a}}{a}$  is the Hubble parameter,  $c$  the velocity of the light and the dot stands for the time derivative.

Combining these two equations leads to

$$(\dot{H}^{-1}) = \frac{3}{2}(\gamma + (1 + \omega - \gamma)\Omega_\Lambda), \quad (6)$$

where the dimensionless density parameter  $\Omega_\Lambda \equiv \Lambda c^2/3H^2$  has been introduced. Eq. (6) is always valid provided the DE is a perfect fluid.

We consider now  $\Lambda$  as a vacuum energy density associated to the FLRW event-horizon such as

$$\Lambda = \frac{3\alpha^2}{r^2}, \quad (7)$$

where  $r$  is the proper radius of the event-horizon, and  $\alpha$  is a dimensionless constant parameter. This form of  $\Lambda$  was previously obtained by [16,17] when  $\alpha = 1$ , and by [18] when  $\alpha \neq 1$ .

Using the quantity  $\Omega_\Lambda$ , relation (7) becomes

$$\sqrt{\Omega_\Lambda} = \frac{\alpha c}{rH}. \quad (8)$$

The proper radius of the flat FLRW event-horizon is

$$r(t) = a(t) \int_t^\infty \frac{c dt'}{a(t')}. \quad (9)$$

The derivative of (9) with respect to time gives

$$H - \frac{\dot{r}}{r} = \frac{c}{r}. \quad (10)$$

For convenience, we introduce the variable  $x \equiv \ln a(t)$  such as  $x = 0$  today. Relation (10) becomes then

$$1 - \frac{r'}{r} = \frac{c}{rH} = \frac{\sqrt{\Omega_\Lambda}}{\alpha} \left( r' \equiv \frac{dr}{dx} \right), \quad (11)$$

where the prime means the derivative with respect to  $x$ .

In the same manner, we can rewrite relation (6)

$$\frac{(\frac{1}{H})'}{(\frac{1}{H})} = \frac{3}{2}(\gamma + (1 + \omega - \gamma)\Omega_\Lambda). \quad (12)$$

Finally, by combining Eqs. (11) and (12) with the derivative of Eq. (8), one obtains

$$\Omega'_\Lambda = \Omega_\Lambda \left\{ 3[\gamma + (1 + \omega - \gamma)\Omega_\Lambda] - 2 \left[ 1 - \frac{\sqrt{\Omega_\Lambda}}{\alpha} \right] \right\}. \quad (13)$$

Let us emphasize that this equation is valid for any values of  $\gamma$  (constant) and  $\omega$  (constant or variable), independently of the fact that the two components  $\rho$  and  $\rho_\Lambda$  are interacting or not.

It is useful to derive from the field equations (4) and (5) the deceleration parameter  $q$

$$q \equiv \frac{-\ddot{a}}{aH^2} = \frac{1}{2}[(3\gamma - 2) + 3(\omega + 1 - \gamma)\Omega_\Lambda] \quad (14)$$

which is valid in the two models.

In the following, we assume that the “matter” component  $\rho$  is dust ( $\gamma = 1$ ), so that (13) and (14) become

$$\Omega'_\Lambda = \Omega_\Lambda \left( 1 + 2 \frac{\sqrt{\Omega_\Lambda}}{\alpha} + 3\omega\Omega_\Lambda \right), \quad (15)$$

$$q = \frac{1}{2}(1 + 3\omega\Omega_\Lambda). \quad (16)$$

The relations (1)–(16), as well as the energy–momentum conservation law  $\nabla_\beta T^{\alpha\beta} = 0$  (or, equivalently, the Bianchi identity), are valid in the two models under

consideration, which we denote  $\Lambda(t)CDM$  models hereafter.

From now on, the assumptions of the ehT model will be different from those of the LHG model.

### 3. Model with interacting components

In the ehT model, we assume that the DE component satisfies thermodynamical state equations, i.e., relations between its thermodynamical variables which are valid in any space–time. Therefore, any thermodynamical state equation valid in the de Sitter’s space–time [15,24]—for instance,  $P_\Lambda = -\rho_\Lambda$  or  $\rho_\Lambda = 12\pi^2 T_\Lambda^2$  ( $T_\Lambda$  the temperature)—remains valid in the FLRW space–time. Thus, if the DE is an actual cosmological component, its thermodynamical state equations will stay the same independently on the choice of the space–time, as well as for any other component. Now, the DE energy density in the de Sitter space–time, as cosmological constant, satisfies the state equation (3) with  $\omega = -1$ .

Then, the energy conservation law  $u_\alpha \nabla_\beta T^{\alpha\beta} = 0$  leads to the two following alternatives:

- (i) Either, the energy of each component is conserved separately and, of course,  $\Lambda$  has to be constant.
- (ii) Or, more generally, the components’ energies are only conserved together,  $\Lambda = \Lambda(t)$  is then possible.

The ehT model assumes the point (ii), which supposes an interaction between the matter and the DE. In the same vein, other models assuming an interaction between the DE and dark matter (DM) components of the cosmic fluid were recently studied (e.g., [25–27]).

This suggests to retain the relation (7) which is valid in the de Sitter’s space–time when  $\alpha = 1$ . In Section 5, some consequences of the presence of the parameter  $\alpha$  in the ehT and LHG models are discussed. Using the holographic principle can lead also to choose the relation (7) [17,18]. These two last references assume a variable state equation ( $\omega = \omega(x)$ ) for the DE, and independent energy conservation laws for the matter and DE components. Conversely, the present model assumes  $\omega = -1$  (vacuum), and that the energy conservation is only valid for the two components considered together.

Eq. (15) can be rewritten

$$\Omega'_\Lambda = 3\Omega_\Lambda(\beta_2 - \sqrt{\Omega_\Lambda})(\beta_1 + \sqrt{\Omega_\Lambda}) \quad (17)$$

where the constants  $\beta_1$  and  $\beta_2$  are given by

$$\begin{aligned} \beta_1 &\equiv \frac{1}{3\alpha}(\sqrt{1+3\alpha^2} - 1), \\ \beta_2 &\equiv \frac{1}{3\alpha}(\sqrt{1+3\alpha^2} + 1), \quad \beta_1, \beta_2 > 0. \end{aligned} \quad (18)$$

By setting  $\alpha = 1$ , Eq. (17) becomes

$$\Omega'_\Lambda = \Omega_\Lambda(1 - \sqrt{\Omega_\Lambda})(3\sqrt{\Omega_\Lambda} + 1), \quad (19)$$

which differs from Eq. (8) in [18]. Nevertheless a straightforward calculation (using (12), (15) and the derivative of the definition of  $\Omega_\Lambda$ ) gives

$$\Lambda' = 2\Lambda(\sqrt{\Omega_\Lambda} - 1), \quad (20)$$

which is common to the two models. As  $\Lambda'$  is always negative,  $\Lambda$  is decreasing with time. Observational evidences provide a very small present value for  $\rho_\Lambda$  (fine-tuning problem) and of the same order as  $\rho$  (coincidence problem).

Introducing the function  $y(x) \equiv \sqrt{\Omega_\Lambda}$ , relation (17) becomes

$$2y' = 3y(\beta_2 - y)(\beta_1 + y). \quad (21)$$

Its solution is (in the only case considered here where  $y < \beta_2$ )

$$K_1 a = \frac{y^2}{(\beta_2 - y)^{\frac{\alpha}{\beta_2\sqrt{1+3\alpha^2}}} (\beta_1 + y)^{\frac{\alpha}{\beta_1\sqrt{1+3\alpha^2}}}}. \quad (22)$$

$K_1$  is a constant of integration which can be related to the initial condition  $y_0 = \sqrt{\Omega_\Lambda^0}$ .

We derive now the expression of  $r = r(y)$ . Using Eqs. (11) and (21) yields

$$d(\ln r) = dx - \frac{2dy}{3\alpha(\beta_2 - y)(\beta_1 + y)}. \quad (23)$$

After integration, one obtains

$$K_2 r = a \left( \frac{\beta_2 - y}{\beta_1 + y} \right)^{\frac{1}{\sqrt{1+3\alpha^2}}} \quad (24)$$

or equivalently

$$K r = \frac{y^2}{(\beta_2 - y)^{\frac{\alpha-\beta_2}{\beta_2\sqrt{1+3\alpha^2}}} (\beta_1 + y)^{\frac{\alpha+\beta_1}{\beta_1\sqrt{1+3\alpha^2}}}},$$

$$K \equiv K_1 K_2. \quad (25)$$

$K_2$  is a second constant of integration which depends on  $y_0$  and  $r_0 = \alpha c(y_0 H_0)^{-1}$ . The expressions of  $K_1$  and  $K_2$  depend explicitly on the two priors  $\Omega_\Lambda^0$  and  $H_0$ . The current values of  $\Omega_\Lambda^0$  and  $H_0$  are  $\Omega_\Lambda^0 = 0.7$  and  $H_0 = 72 \text{ km s}^{-1} \text{ Mpc}^{-1}$  [28]. With these two numerical values, it is interesting to deal with the case where  $\alpha = 1$  for which  $\beta_1 = \frac{1}{3}$  and  $\beta_2 = 1$ . One obtains

$$\begin{aligned} K_1 a &= \frac{y^2}{(1-y)^{\frac{1}{2}} \left(\frac{1}{3} + y\right)^{\frac{3}{2}}}, \\ K_1 &\equiv \frac{y_0^2}{(1-y_0)^{\frac{1}{2}} \left(\frac{1}{3} + y_0\right)^{\frac{3}{2}}} = 1.3686, \end{aligned} \quad (26)$$

$$K_2 r = a \left( \frac{1-y}{\frac{1}{3} + y} \right)^{1/2}, \quad \text{or} \quad K r \equiv \left( \frac{y}{\frac{1}{3} + y} \right)^2,$$

$$r_0 = \frac{c}{H_0 y_0} = 4980.12 \text{ Mpc},$$

$$K_2 \equiv \frac{1}{r_0} \left( \frac{1-y_0}{\frac{1}{3} + y_0} \right)^{1/2} = 7.50265 \times 10^{-5} \text{ Mpc}^{-1},$$

$$K = 1.02681 \times 10^{-4} \text{ Mpc}^{-1}. \quad (27)$$

However the previous values of  $H_0$  and  $\Omega_\Lambda^0$  are model-dependent. They were obtained in the framework of the  $\Lambda$ CDM model. We shall see that starting with the same observational SNIa data, the best fit to the  $\Lambda(t)$ CDM models give appreciably different central values of  $H_0$  and  $\Omega_\Lambda^0$ .

#### 4. SNIa constraints on the ehT model

In order to compare these theoretical results with the observations of the SNIa magnitudes, the luminosity distance  $d_L$  has to be expressed with respect to the redshift  $z = a^{-1} - 1$ . In the ehT model, it yields

$$\begin{aligned} d_L &= (1+z)[(1+z)r - r_0] \\ &= \frac{c(1+z)}{y_0 H_0} \left[ (1+z) \frac{r}{r_0} - 1 \right], \end{aligned} \quad (28)$$

where the expression of  $r$  depends on  $z$ . As before, we only consider the case  $\alpha = 1$ . Both Eqs. (22) and (25) give a parametric representation (via the ‘‘parameter’’  $y$ ) of  $r$  as function of  $z$ . Indeed, (22) yields immediately  $z = z(y)$  (with  $a = (1+z)^{-1}$ ).

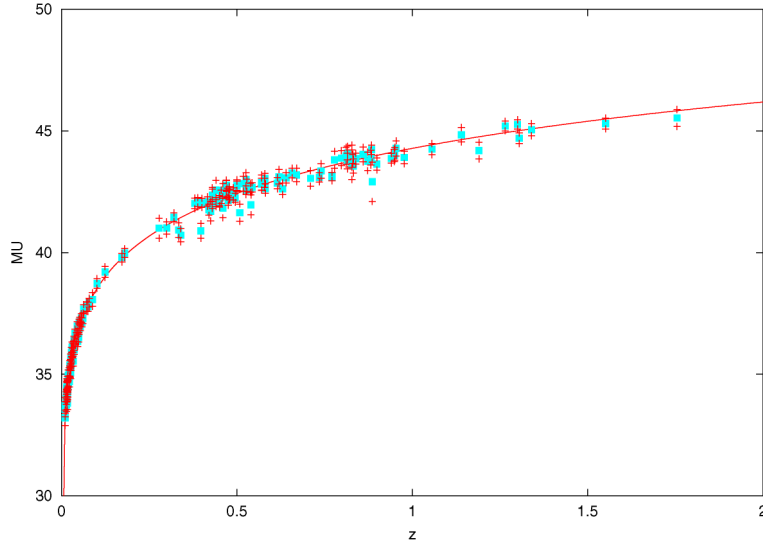


Fig. 1. The “distance moduli”  $\mu(z)$  of the ehT model.

The set of the theoretical curves “distance moduli”  $\mu$  versus the redshift  $z$ ,

$$\mu \equiv m - M = 25 + 5 \log_{10}(d_L), \quad (29)$$

with  $d_L$  in Mpc,

predicted by the model parametrized by the two cosmological parameters  $y_0 = \sqrt{\Omega_\Lambda^0}$  and  $H_0$ , can be plotted. For the two parameters  $\Omega_\Lambda^0$  and  $H_0$  free, the best fit to the magnitude observational data of the 157 SnIa “Gold sample” [23] can be determined by minimizing the function  $\chi^2 = \sum (\frac{\mu(z) - \mu_i(z_i)}{\sigma_i})^2$ , where  $\mu_i(z_i)$  denotes the values of the magnitude for the observational data,  $\sigma_i$  the corresponding error and the summation is taken over any of the 157 data of the sample. The corresponding values of  $\Omega_\Lambda^0$  and  $H_0$  are derived by numerical computation. More precisely, Eq. (21) is integrated by the method of Runge–Kutta of order 4, and the expression of  $z(y)$  is deduced by use of (22). With the help of Eqs. (28) and (29), the values of  $\mu(z)$  for  $z$  ranging from 0 to 100 are then obtained. After a simple numerical evaluation of  $\chi^2$  for  $\Omega_\Lambda^0$  ranging from 0 to 1 and  $H_0$  from 50 to 100, the best fit corresponding to  $\chi^2 = 178, 7$  is obtained for

$$H_0 = 64_{-4}^{+7} \text{ km s}^{-1} \text{ Mpc}^{-1}, \quad \Omega_\Lambda^0 = 0.63_{-0.01}^{+0.1}. \quad (30)$$

The function  $\mu(z)$  is plotted in Fig. 1 for  $z$  ranging from 0 to 2.

The likelihood function  $\mathcal{L}(\Omega_\Lambda^0)$  (see Fig. 2) is derived by marginalization of  $H_0$  and furnishes the same value of the parameter  $\Omega_\Lambda^0$ .

Finally, the deceleration parameter  $q$  can be expressed as a function of  $y$  in the ehT model (for  $\alpha = 1$ ) from Eq. (16) (with  $\omega = -1$ )

$$q = \frac{1}{2}(1 - 3y^2). \quad (31)$$

In Fig. 3 the curve  $q(z)$  of the ehT model is plotted. Today the deceleration is  $q_0 = -0.445$ , and the deceleration–acceleration transition occurred at  $z_T \simeq 0.965$ .

## 5. The event horizon and the parameter $\alpha$

We examine here the influence of the parameter  $\alpha$  on the limits of the proper radius  $r$  of the event horizon (eh) in the two models. First, let us consider the LHG model.

By comparison with the relations (22) and (25) of the ehT model, the LHG model would lead to the relations ( $a$  is given by (9) of [18] and  $r$ , not explicitly

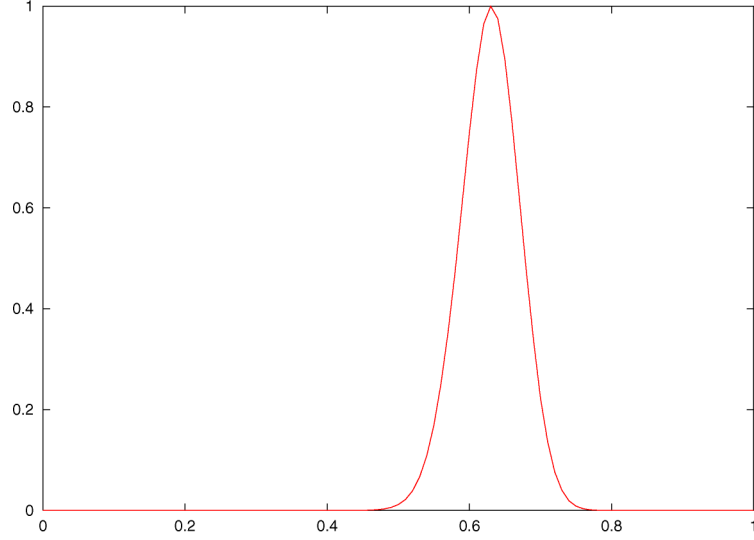


Fig. 2. The likelihood function  $\mathcal{L}(\Omega_A^0)$  of the ehT model.

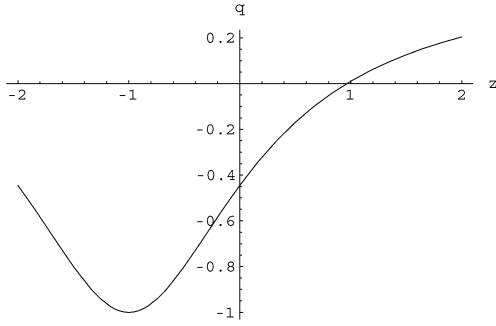


Fig. 3. The deceleration parameter  $q(z)$  of the ehT model.

given, can be deduced from their Eqs. (6) and (9):

$$Y_0 a = \frac{y^2(1+y)^{\frac{\alpha}{2-\alpha}}}{(1-y)^{\frac{\alpha}{2+\alpha}}(\alpha+2y)^{\frac{8}{4-\alpha^2}}}, \quad \alpha \neq 2,$$

$$Y_0 \equiv \frac{y_0^2(1+y_0)^{\frac{\alpha}{2-\alpha}}}{(1-y_0)^{\frac{\alpha}{2+\alpha}}(\alpha+2y_0)^{\frac{8}{4-\alpha^2}}}, \quad (32)$$

$$r = \frac{\alpha}{Y_0^{\frac{3}{2}} H_0 \sqrt{1-\Omega_A^0}} \frac{y^2(1+y)^{\frac{1+\alpha}{2-\alpha}}(1-y)^{\frac{1-\alpha}{2+\alpha}}}{(\alpha+2y)^{\frac{12}{4-\alpha^2}}}. \quad (33)$$

For  $\alpha = 2$ , the LHG model requires to start again the calculation from the differential equation (15) which becomes:

$$2y' = y(1-y)(1+y)^2. \quad (34)$$

Its integration yields

$$a = \frac{(1-y_0)^{\frac{4}{3}}(1+y_0)^{\frac{2}{3}}}{y_0^2} \frac{y^2}{(1-y)^{\frac{4}{3}}(1+y)^{\frac{2}{3}}} \times \exp\left(\frac{8}{3}\left(\frac{1}{1+y} - \frac{1}{1+y_0}\right)\right). \quad (35)$$

Then,

$$r = \frac{2c(1-y_0)^2(1+y_0)}{H_0 \sqrt{1-\Omega_A^0} y_0^3} \frac{y^2 \exp\left(\frac{4}{1+y} - \frac{4}{1+y_0}\right)}{(1-y)^{\frac{3}{2}}(1+y)^{\frac{1}{2}}}. \quad (36)$$

We can see from (32) or (35) that  $a$  tends to infinity when  $y$  tends to 1, for any values of  $\alpha$  (positive, see (8)). But the behaviour of  $r$  differs because it depends on the parameter  $\alpha$ , as it can be seen from (33) and (36). Three cases can be distinguished for the behaviour of  $r$  in the limit  $y \rightarrow 1$ :

$$r \rightarrow 0 \quad \text{if } \alpha < 1, \quad (37)$$

$$r \rightarrow \infty \quad \text{if } \alpha > 1, \quad (38)$$

$$r \rightarrow r_i = cst = \left(\frac{2}{9}\right)^2 \frac{c}{H_0 \sqrt{1-\Omega_A^0} Y_0^{\frac{3}{2}}} = r_0 \left(\frac{2(1+2y_0)^2}{9(1+y_0)y_0}\right)^2 \equiv \frac{c}{H_i} \quad \text{if } \alpha = 1. \quad (39)$$

The first two cases (i.e.,  $r \rightarrow 0$  and  $r \rightarrow \infty$ ) disagree with the holographic point of view, because they

would prevent any cut-off (IR and UV, respectively). In particular, the case  $\alpha < 1$  seems to be proscribed because it could not prevent the singularity formation and would correspond to the absence of black hole formation.

The third case only ( $\alpha = 1$ ) corresponds to a de Sitter asymptotic limit. In Eq. (39), the index  $i$  of  $H$  means exponential “inflation”. Note that the limit  $\frac{r_i}{r_0}$  depends only on  $y_0$ , and its value is:  $\frac{r_i}{r_0} = 1.06813$  if we take  $y_0 = \sqrt{0.7}$ . As  $r_0 = \frac{c}{H_0 y_0} = 4980.12$  Mpc,  $r_i$  is equal to 5319.42 Mpc. The expression of  $r_0$  is formally the same in the two models and depends only on the choice of the observational priors  $H_0$  and  $y_0$ . However, each model leading to slightly different adjustments of these parameters gives slightly different values of  $r_0$  and  $r_i$  then.

In the case of the ehT model, for any arbitrary  $\alpha$ , the same phenomenon appears and the value  $\alpha = 2$  does not necessitate a special study. In the limit  $y \rightarrow 1$ , Eqs. (22) and (25) give

$$a \rightarrow \infty \quad \text{and} \quad r \rightarrow 0 \quad \text{if} \quad \alpha < 1$$

(equivalently,  $\beta_2 > 1$ )

$$a \rightarrow \infty \quad \text{and} \quad r \rightarrow cst = \frac{1}{K} \left( \frac{3}{4} \right)^2 = 5478.13 \text{ Mpc}$$

if  $\alpha = 1$  (equivalently,  $\beta_2 = 1$ ).

When  $\alpha > 1$ ,  $\beta_2 < 1$ , then  $y \rightarrow \beta_2$  before reaching 1, and  $a \rightarrow \infty$ , while  $r \rightarrow \infty$  for this asymptotical limit  $\beta_2$  of  $y$ . From the today observational evaluations,  $\beta_2$  has to be  $> \sqrt{0.63} = 0.79$ , and so  $\alpha < \frac{2\sqrt{0.63}}{3 \times 0.63 - 1} = 1.78$ . In the future,  $\alpha$  range from 1 to 1.78 will become more and more narrow, tending to 1, as long as Eq. (17) of the model, indicating a growth of  $\Omega_\Lambda$ , remains valid.

Thus, the case  $\alpha = 1$  appears to us as the most attractive. The corresponding de Sitter’s limit is  $r_i = 5478.13$  Mpc. It is a little greater than the limit of the LHG model (5319.42 Mpc), which means a little weaker exponential inflation.

## 6. Conclusion

We have seen that the form  $\Lambda \sim r^{-2}$  of the ehT model [16] for the DE, clearly also supported by the holographic principle [17,18], leads, in our study, to

two somewhat different models, owing to the chosen energy conservation equation. In the ehT model,  $\alpha = 1$  and the best fit ( $\chi^2_v = 1.14$ ) to the SnIa’s data from the “gold” sample [23] gives us  $H_0 = 64 \text{ km Mpc}^{-1} \text{ s}^{-1}$  and  $\Omega_\Lambda^0 = 0.63$ . If  $\alpha \neq 1$  (as in the LHG model) it is worth observing that the  $\alpha < 1$  values are not very attractive because they lead to the singularity  $r \rightarrow 0$  when  $\Omega_\Lambda \rightarrow 1$ .

For the deceleration–acceleration transition epoch we find a redshift  $z_T = 0.96$ , a value slightly higher than the ones recently published ( $0.28 \leq z_T \leq 0.72$ ) [18,23] and very sensitive to the  $\Omega_\Lambda^0$  value. Comparing the values of the cosmological parameters in various models requires to discuss not only the choice of the parameter  $\alpha$  but also the forms or relations taken for  $q(z)$  (for instance,  $q(z) = q_0 + q_1 z$  valid when  $z \ll 1$ ), for  $\omega(z)$ , or for  $d_L(z)$ . Besides, in a given model, one has to take into account the energy conservation laws for DM and DE. In most cases, the authors assume an energy conservation law for each component separately. Here we have considered the more general situation of a global conservation of the whole energy and so, necessarily, an interaction between DM and DE. Such an interaction could induce higher values for the transition redshift  $z_T$ , as noted by Amendola et al. for models with coupling [29,30]. Future observations in the high redshift range could allow to discriminate between theories with coupled components and theories with distinct conservation laws.

## References

- [1] A.G. Riess, Astron. J. 116 (1998) 1009.
- [2] S. Perlmutter, et al., Nature 391 (1998) 51.
- [3] B. Ratra, P.J.E. Peebles, Phys. Rev. D 37 (1988) 3406.
- [4] G.L. Murphy, Phys. Rev. D 8 (1973) 4231.
- [5] K. Freese, F.C. Adams, J.A. Frieman, Nucl. Phys. B 287 (1987) 797.
- [6] M. Özer, M.O. Taha, Nucl. Phys. B 287 (1987) 776.
- [7] W. Chen, Y.S. Wu, Phys. Rev. D 41 (1990) 695.
- [8] J.C. Carvalho, J.A.S. Lima, I. Waga, Phys. Rev. D 46 (1992) 2404.
- [9] J.A.S. Lima, J.M.F. Maia, Phys. Rev. D 49 (1994) 5597.
- [10] E. Gunzig, R. Maartens, A. Nesteruk, Class. Quantum Grav. 15 (1998) 923.
- [11] I. Prigogine, J. Gehehiau, E. Gunzig, P. Nardone, Gen. Relativ. Gravit. 21 (1989) 767.
- [12] P.C.W. Davies, Class. Quantum Grav. 5 (1988) 1341.
- [13] M.D. Pollock, T.P. Singh, Class. Quantum Grav. 6 (1989) 901.
- [14] J.D. Bekenstein, Phys. Rev. D 7 (1973) 2333.

- [15] G. Gibbons, S.W. Hawking, *Phys. Rev. D* 15 (1977) 2738.
- [16] J. Gariel, G. Le Denmat, *Class. Quantum Grav.* 16 (1999) 149.
- [17] M. Li, *Phys. Lett. B* 603 (2004) 1.
- [18] Q.G. Huang, Y. Gong, *J. Cosmol. Astropart. Phys.* 08 (2004) 006.
- [19] J.M. Overduin, F.I. Cooperstock, *Phys. Rev. D* 58 (1998) 043506.
- [20] A. Pradhan, G.S. Khadekar, D. Srivastava, *gr-qc/0506112*.
- [21] A.I. Arbab, *J. Cosmol. Astropart. Phys.* 05 (2003) 008.
- [22] S. Ray, U. Mukhopadhyay, *astro-ph/0407295*.
- [23] A.G. Riess, et al., *astro-ph/0402512*.
- [24] M. Gasperini, *Class. Quantum Grav.* 5 (1988) 521.
- [25] D. Pavon, S. Sen, W. Zimdhal, *astro-ph/0402067*.
- [26] G. Olivares, F. Atrio-Barandela, D. Pavon, *astro-ph/0503242*.
- [27] W. Zimdahl, *gr-qc/0505056*.
- [28] D.N. Spergel, et al., *astro-ph/0302209*.
- [29] L. Amendola, *Mon. Not. R. Astron. Soc.* 32 (2003) 221.
- [30] L. Amendola, M. Gasperini, F. Piazza, *astro-ph/0407573*.